THE INSTITUTE OF ELECTRONICS,
INFORMATION AND COMMUNICATION ENGINEERS

IEICE Technical Report

High-Resolution Ultra-Wideband Radar Imaging using Kirchhoff Integral and F-K Migration with Boundary Scattering Transform

Takuya SAKAMOTO

Graduate School of Engineering, University of Hyogo 2167 Shosha, Himeji, 671-2280 Japan

E-mail: t-sakamo@i.kyoto-u.ac.jp

Abstract This paper introduces a fast high-resolution imaging algorithm designed for ultra-wideband radar, and combines modified Kirchhoff migration and frequency-wavenumber (F-K) migration. The proposed algorithm also uses the texture method and inverse boundary scattering transform to calculate efficiently the integral arising in modified Kirchhoff migration, and thus enabling the integral in the F-K domain to be calculated within a short time.

Keywords Kirchhoff migration, frequency-wavenumber migration, texture method, boundary scattering transform

1. Introduction

A high-resolution imaging algorithm called modified Kirchhoff migration has been reported [1]. Originally, the method was used only in the time domain because the modified Kirchhoff integrand varies depending on the candidate target position. We propose here a method that incorporates the texture method [2] and the inverse boundary scattering transform (IBST) [3] to estimate an approximate target position, so that the modified Kirchhoff integrand can be determined. This enables the fast Fourier transform (FFT) to be used and accelerate imaging. The proposed method is applied to measurement data to evaluate its imaging capability.

2. Modified Kirchhoff Migration Imaging

Stolt frequency-wavenumber (F-K) migration is known to be a fast imaging method, and has been studied in numerous works [4–6]. The method uses back-projection in the F-K domain, meaning that Stolt F-K migration is basically the same as delay-and-sum migration [7]. The image resolution therefore is no better than that of many conventional imaging algorithms.

Zhuge et al. [1] proposed an imaging algorithm, based on a multiple-input multiple-output radar model. They calculated the Kirchhoff migration image using double integrals over the transmitter and receiver scan surfaces. Although the present study assumes the use of a single-input single-output radar system that uses a pair of antennas with a fixed spacing, the same formula is applicable. In our system, the transmitter and receiver are located at $\boldsymbol{r}_1$ and $\boldsymbol{r}_2$, respectively, with a midpoint of $\boldsymbol{r}_0$ at a fixed spacing $2d$ in the x-direction. Let us redefine the raw signal $s_0(\boldsymbol{r}_0,t)$ that is transmitted and received at $\boldsymbol{r}_1=\boldsymbol{r}_0-\boldsymbol{d}$ and $\boldsymbol{r}_2=\boldsymbol{r}_0+\boldsymbol{d}$, respectively, where $\boldsymbol{d}=(d,0,0)$. This raw signal can also be expressed as $s(X,Y,Z)$. Kirchhoff migration [8] involves performing an integration of the signals to obtain image $I(\boldsymbol{r})$ in the form

$$I(x)=\int_S \frac{\partial R_1}{\partial n}\frac{\partial R_2}{\partial n}\frac{1}{R_1R_2} \cdot\left\{\frac{1}{c^2}\frac{\partial^2}{\partial t^2}s_0(\boldsymbol{r}_0,t+\tau)+\frac{1}{c}\left(\frac{1}{R_1}+\frac{1}{R_2}\right)\frac{\partial}{\partial t}s_0(\boldsymbol{r}_0,t+\tau) +\frac{1}{R_1R_2}s_0(\boldsymbol{r}_0,t+\tau)\right\}\mathrm{d}S\Bigg|_{t=0}, \quad (1)$$

where S is the antenna scanning plane z=0, $R_1=|\boldsymbol{r}-\boldsymbol{r}_1|$, $R_2=|\boldsymbol{r}-\boldsymbol{r}_2|$, $\tau=(R_1+R_2)/c$, and $\partial/\partial n$ denotes the spatial derivatives normal to the surface S. Equation (1) indicates that Kirchhoff migration needs only a single integration, unlike the formula proposed in [1].

The integral in Eq. (1) can be readily calculated in the space-time domain [1]. This is because the region of interest is divided into numerous voxels, and we can calculate all necessary coefficients, such as R_1 and R_2 in Eq. (1), for each of these voxels without estimating the actual target position. This method is what is called Kirchhoff migration.

Note here that Eq. (1) can be converted to the frequency domain by introducing the appropriate frequency domain kernel, as used in the diffraction tomographic algorithm [9]. Using a fundamentally different principle, this paper provides an alternative approach to this problem. In future studies, we shall compare image resolution and computational speed achieved by the diffraction tomographic algorithm and the algorithm proposed in this paper.

3. Inverse Boundary Scattering Transform and Texture Angles

We have developed a fast radar imaging algorithm

(SEABED for shape estimation algorithm based on the boundary scattering transform and extraction of directly scattered waves) that uses the IBST. This transform develops a one-to-one correspondence between a target shape and the corresponding echo data and hence is reversible [10–13]. SEABED does not require any iterative or repetitive processing, and thus enables fast imaging. Another advantage of SEABED is that, unlike conventional methods, a target location is estimated for each radar image pixel. In this study, we exploit this characteristic to develop a new algorithm.

A radar image can be obtained using the following IBST [14, 15], which is applied to signal $s(X, Y, Z)$:

$$\begin{cases} x = X - \dfrac{2Z^3 Z_X}{Z^2 - d^2 + \sqrt{(Z^2-d^2)^2 + 4d^2Z^2{Z_X}^2}}, \\ y = Y + Z_Y\left\{d^2(x-X)^2 - Z^4\right\}/Z^3, \\ z = \sqrt{Z^2 - d^2 - (y-Y)^2 - \dfrac{(Z^2-d^2)(x-X)^2}{Z^2}} \end{cases}, \quad (2)$$

where, for simplicity in notation, $Z_X = \partial Z/\partial X$ and $Z_Y = \partial Z/\partial Y$. In the original SEABED, the signal peaks are extracted, and the IBST is applied to these peaks. However, in this study, we require the target locations corresponding to all the pixels in the radar image.

We introduce the texture angle for radar images to estimate the derivatives Z_X and Z_Y that are required in Eq. (2). The texture angle was originally proposed for the estimation of target speeds from radar signals [16, 17]. We use the same concept but for a different purpose: we define the texture angle of a radar signal $s(X, Y, Z)$ as

$$\theta_X(X,Y,Z) = \tan^{-1}\left(\frac{\partial s(X,Y,Z)/\partial X}{\partial s(X,Y,Z)/\partial Z}\right), \quad (3)$$

$$\theta_Y(X,Y,Z) = \tan^{-1}\left(\frac{\partial s(X,Y,Z)/\partial Y}{\partial s(X,Y,Z)/\partial Z}\right), \quad (4)$$

The derivatives Z_X and Z_Y that are needed for the IBST are estimated using these values θ_X and θ_Y.

Let us assume that s(X, Y, Z) can be approximated as s(X, Y, Z)=$p(Z-Z_0(X, Y))$, which means that the signal has a local equiphase surface $Z=Z_0(X, Y)$. Under this assumption, we obtain

$$\begin{aligned} &s(X,Y,Z) = p(Z - Z_0(X,Y)) \\ &\partial s/\partial X = \partial Z_0/\partial X \cdot \dot{p}(Z - Z_0(X,Y)) \quad (5) \\ &\partial s/\partial Z = \dot{p}(Z - Z_0(X,Y)) \end{aligned}$$

Therefore, $Z_X=\partial Z_0/\partial X$ and $Z_Y=\partial Z_0/\partial Y$ can be obtained by calculating $Z_X=-\tan(\theta_X)$ and $Z_Y=-\tan(\theta_Y)$. Using these results, we can estimate the target position (x, y, z) using Eq. (2). The texture angles θ_X and θ_Y correspond to the angles of the stripes that appear in the X-Z and Y-Z planes. These stripes are intersections of the equiphase surface Z with the XoZ or YoZ planes.

Next, the estimated target position (x, y, z) is used to calculate

$$R_1 = \sqrt{(x - X + d)^2 + (y-Y)^2 + z^2}, \quad (6)$$

$$R_2 = \sqrt{(x - X - d)^2 + (y-Y)^2 + z^2}, \quad (7)$$

and $\partial R_1/\partial n=z/R_1$, $\partial R_2/\partial n=z/R_2$. These values are then substituted into the following equation to give the modified Kirchhoff signal:

$$\begin{aligned} s_m{}'(\boldsymbol{r}_0,t) = \frac{\partial R_1}{\partial n}\frac{\partial R_2}{\partial n}\frac{1}{R_1R_2}\cdot\Bigg\{&\frac{1}{c^2}\frac{\partial^2}{\partial t^2}s_0(\boldsymbol{r}_0,t) \\ &+\frac{1}{c}\left(\frac{1}{R_1}+\frac{1}{R_2}\right)\frac{\partial}{\partial t}s_0(\boldsymbol{r}_0,t) + \frac{1}{R_1R_2}s_0(\boldsymbol{r}_0,t)\Bigg\} \end{aligned}. \quad (8)$$

Finally, as proposed in [1], we can compensate for the propagation path loss using $s_m=R_1^2R_2^2s'_m$. Kirchhoff migration can then be realized by simply applying a conventional migration to the modified Kirchhoff signal $s_m(\boldsymbol{r}_0,t)$ rather than the original signal $s(\boldsymbol{r}_0,t)$. This can be calculated using the FFT in exactly the same manner as used for Stolt F-K migration. The use of texture angles and the IBST enables using both Stolt F-K migration and Kirchhoff migration simultaneously, which means that we can obtain high-quality images in a shorter time. We only use texture angles and the IBST in our proposed hybrid method, and not in other conventional methods.

4. Proposed Method

In this section, the actual procedure used for the proposed method is explained.

1) Calculate the texture angles $\theta_X(X_i, Y_i, Z_i)$ and $\theta_Y(X_i, Y_i, Z_i)$ using Eqs. (3) and (4), respectively, for each data sample \$s(X_i, Y_i, Z_i) (i=1,2,…,N), where N is the number of data points and is defined as $N=N_XN_YN_t$. Here, N_X and N_Y are the numbers of measurement points in the x and y directions, respectively, and N_t is the number of time samples.
2) Obtain the partial derivatives $Z_X=-\tan(\theta_X)$ and $Z_Y=-\tan(\theta_Y)$, and apply the IBST as per Eq. (2) to calculate the target position (x_i, y_i, z_i) for the i-th data sample.
3) Calculate $\partial R_1/\partial n=z/R_1$, $\partial R_2/\partial n=z/R_2$ for each estimated reflection point (x_i, y_i, z_i).
4) Generate the modified Kirchhoff signals $s_m(X_i, Y_i, Z_i)$ using Eq. (8).
5) Apply Stolt F-K migration to obtain the target image.

Before application of the FFT and the inverse FFT, we apply the Hann window, which is also called a raised cosine window, to suppress undesired components caused by truncation of data. This means that we apply a three-dimensional Hann window twice in the calculation of the Kirchhoff migration and the proposed method. For the examples used in this paper, the roll-off factor of the window is set to 0.3. Some details of this approach are also found in [18].

5. Resolution Improvement using the Proposed Method

We measured radar signals using a network analyzer (PNA E8364B, Keysight Technologies, CA) to sweep from 4.0 to 20.0 GHz. Two Vivaldi antennas were used with antenna separation of 5.5 cm. We used a stainless-steel circular plate (24.0 cm in diameter) patterned with a Siemens star as a target. Both antennas scanned over a square of side length 50.0 cm at 1.0-cm intervals. Figures 1 and 2 show two images, one calculated using conventional frequency-wavenumber (F-K) migration and the other using the proposed method. Using an Intel Xeon E5-2650 v2 processor, the calculation times were 2.48 and 4.49 s, respectively. The image in Fig. 2 has a higher resolution than that in Fig. 1. The respective resolutions, 1.34 and 0.73 cm, indicated an improvement of 1.84 times for the proposed method.

Acknowledgments

This study was supported in part by the SPIRITS Program, JSPS KAKENHI (Grant Numbers 25249057 and 15K18077), and the R&D Project for Expansion of Radio Spectrum Resources for More Efficient Use of Frequency Resources for the Future (The Ministry of Internal Affairs and Communications, Japan).

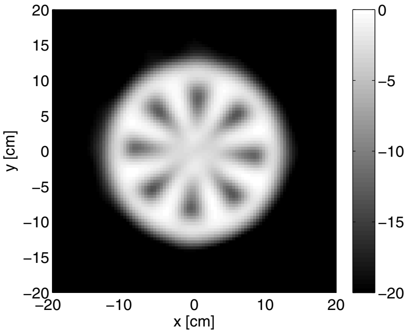

Fig. 1 Image obtained using F-K migration (2.48 s).

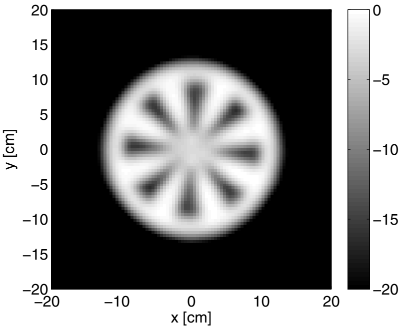

Fig. 2 Image obtained using the proposed method (4.49 s).

References

[1] X. Zhuge, A. G. Yarovoy, T. Savelyev, L. Ligthart, Modified Kirchhoff migration for UWB MIMO array-based radar imaging, IEEE Transactions on Geoscience and Remote Sensing, vol.48, no.6, pp.2692-2703, 2010.

[2] T. Sakamoto, T. Sato, P. J. Aubry, and A. G. Yarovoy, Texture-based automatic separation of echoes from distributed moving targets in UWB radar signals, IEEE Trans. on Geoscience and Remote Sensing, vol.53, no.1, pp.352-361, 2015.

[3] T. Sakamoto, A fast algorithm for 3-dimensional imaging with UWB pulse radar systems, IEICE Transactions on Communications, vol.E90-B, no.3, pp.636-644, March 2007.

[4] X. Xu, E. L. Miller, C. M. Rappaport, Minimum entropy regularization in frequency-wavenumber migration to localize subsurface objects, IEEE Transactions on Geoscience and Remote Sensing, vol.41, no.8, pp.1804-1812, August 2003.

[5] J.-G. Zhao, M. Sato, Radar Polarimetry Analysis Applied to Single-Hole Fully Polarimetric Borehole Radar, IEEE Transactions on Geoscience and Remote Sensing, vol.44, no.12, pp.3547-3554, December 2006.

[6] D. Garcia, L. L. Tarnec, S. Muth, E. Montagnon, J. Por´ee, G. Cloutier, Stolt's f-k migration for plane wave ultrasound imaging, IEEE Transactions on Ultrasonics, Ferroelectrics and Frequency Control, vol.60, no.9, pp.1853-1867, September 2013.

[7] C. Gilmore, I. Jeffrey, and J. Lovetri, Derivation and comparison of SAR and frequency-wavenumber migration within a common inverse scalar wave problem formulation, IEEE Transactions on Geoscience and Remote Sensing, vol.44, no.6, pp.1454-1461, June 2006.

[8] J. A. Stratton, Electromagnetic Theory, Wiley-IEEE Press, Hoboken, NJ, 2007.

[9] W. Zhang and A. Hoorfar, Three-dimensional real-time through the wall radar imaging with diffraction tomographic algorithm, IEEE Transactions on Geoscience and Remote Sensing, vol.51, no.7, 2013.

[10] T. Sakamoto, A fast algorithm for 3-dimensional imaging with UWB pulse radar systems, IEICE Transactions on Communications, vol.E90-B, no.3, pp.636-644, March 2007.

[11] D. W. Winters, J. D. Shea, E. L. Madsen, G. R. Frank, B. D. Van Veen, S. C. Hagness, Estimating the Breast Surface Using UWB Microwave Monostatic Backscatter Measurements, IEEE Transactions on Biomedical Engineering, vol.55, no.1, pp.247-256, January 2008.

[12] S. Hantscher, A. Reisenzahn, C. G. Diskus, Through-Wall Imaging With a 3-D UWB SAR Algorithm, IEEE Signal Processing Letters, vol.15, pp.269-272, February 2008.

[13] R. Salman, I. Willms, "In-Wall Object Recognition based on SAR-like Imaging by UWB-Radar," Proc. 8th European Conference on Synthetic Aperture Radar (EUSAR), June 2010.

[14] S. Kidera, Y. Kani, T. Sakamoto, T. Sato, A fast and high-resolution 3-D imaging algorithm with linear array antennas for UWB pulse radars, IEICE Transactions on Communications, vol.E91-B, no.8, pp.2683-2691, August 2008.

[15] T. Sakamoto, T. G. Savelyev, P. J. Aubry, and A. G. Yarovoy, "Revised Range Point Migration Method for Rapid 3-D Imaging with UWB Radar," Proc. 2012 IEEE International Symposium on Antennas and Propagation and USNC-URSI National Radio Science Meeting, July 2012.

[16] T. Sakamoto, T. Sato, Y. He, P. J. Aubry, A. G. Yarovoy, "Texture-based technique for separating echoes from people walking in UWB radar signals," Proc. 2013 URSI International Symposium on Electromagnetic Theory (EMTS), pp.119-122, 2013.

[17] T. Sakamoto, T. Sato, P. J. Aubry, and A. G. Yarovoy, Texture-based automatic separation of echoes from distributed moving targets in UWB radar signals, IEEE Trans. on Geoscience and Remote Sensing, vol.53, no.1, pp.352-361, 2015.

[18] T. Sakamoto, T. Sato, P. J. Aubry, and A. G. Yarovoy, Ultra-Wideband Radar Imaging using a Hybrid of Kirchhoff Migration and Stolt F-K Migration with an Inverse Boundary Scattering Transform, IEEE Transactions on Antennas and Propagation, vol.63, no.8, pp.3502-3512, Aug. 2015.